Modeling Relative Wind Speed by Optical Stratification Porosity within the Canopy of a Coastal Protective Forest at Different Stem Densities

Jiao-jun Zhu, Yutaka Gonda, Takeshi Matsuzaki and Masashi Yamamoto

Zhu, J., Gonda, Y., Matsuzaki, T. & Yamamoto, M. 2003. Modeling relative wind speed by optical stratification porosity within the canopy of a coastal protective forest at different stem densities. Silva Fennica 37(2): 189–204.

Wind speed and optical stratification porosity (OSP) were measured at various heights inside a coastal protective forest thinned to different stem densities to assess whether any characteristics of the wind profile in the coastal protective forest could be predicted from OSP. OSP was defined as vertical distribution of the proportion of sky hemisphere not obscured by tree elements inside a forest stand, and was determined for various heights using hemispherical photographic silhouettes on a computer processing system. The distribution of OSP in the coastal forest follows the Lambert-Beer's law with an extinction coefficient (ν). The relative wind speed within the canopy can be described using an exponential form with an attenuation coefficient (α). Variation in relative wind speed was very closely correlated with the distribution of OSP within the canopy. While below the canopy, i.e., in the trunk space, relative wind speed was little correlated with the distribution of OSP because the distribution of OSP was relatively constant there. Therefore, the linear relationships between relative wind speed and OSP and between the two coefficients ν and α were established within the canopy. The results suggest that OSP can be used to predict the wind profile in case of the application within the canopy of the coastal forest.

Keywords coastal protective forest, optical porosity, *Pinus thunbergii*, vertical forest structure, wind speed
Authors' addresses *Zhu*: Qingyuan Station of Forest Ecology, Institute of Applied Ecology, the Chinese Academy of Sciences, No. 72 Wenhua Road, Shenyang 110016, P.R. China; *Zhu* (second affil.), *Gonda, Matsuzaki & Yamamoto*: Faculty of Agriculture, Niigata University, Niigata 950-2181, Japan
Fax +88 24 2384 3313 **E-mail** jiaojun@agr.niigata-u.ac.jp, jiaojunzhu@iae.ac.cn
Received 17 April 2001 **Accepted** 21 January 2003

1 Introduction

Porosity of a windbreak is defined as the ratio or percentage of pore space to the space occupied by tree stems, branches, twigs and leaves (Cao 1983, Jiang et al. 1989, Loeffler et al. 1992). Porosity as the most important characteristic of a windbreak with respect to wind reduction has been recognized (Carborn 1965, Moysey and McPherson 1966, Hagen and Skidmore 1971a, b, Plate 1971, Bean et al. 1975, Zhu and Jiang 1992, Groß 1993). Unfortunately, it is nearly impossible to physically measure the aerodynamic porosity of natural plants because of its three-dimensional nature of the pores through which the wind flows. Therefore, efforts have been made to find an alternative measurement (Loeffler et al. 1992). Optical porosity, a two-dimensional measure of porosity determined from the plant silhouettes, has been proved to be a promising alternative of aerodynamic porosity, especially for the thin windbreaks (Kenney 1987, Heisler and DeWalle 1988, Jiang et al. 1989, 1994, 1999).

Methods for estimating the optical porosity of windbreak have been developed (Bean et al. 1975, Kenney 1987, Jiang et al. 1989, Zhou et al. 1991). Particularly for narrow windbreaks, it can be estimated using digitized photographic silhouettes with very high accuracy (Kenney 1987, Jiang et al. 1989). There are many investigations on the relationships between optical porosity of windbreak and wind reduction (Hagen and Skidmore 1971a, b, Fu et al. 1992, Loeffler et al. 1992, Groß 1993, Jiang et al. 1994, 1999).

When we consider the atmospheric motion in other forests, i.e. not in the shelterbelt or windbreak, for example, a coastal protective forest, it becomes quite apparent that the relationship between airflow and optical porosity in the coastal protective forest is a significant aspect for evaluations of wind reduction, wind damage and other ecological effects of wind (Balckburn and Pett 1988, Peltola and Kellomäki 1993, Ennos 1997, Zhu et al. 1998, Peltola et al. 1999). However, there is little information about porosity for other forests, especially for a coastal protective forest. Obviously, the optical porosity of windbreak does not fit in with the coastal protective forest. It is fair to say that the relationships between wind speed and the optical porosity have been paid little attention in the coastal protective forests because of the difficulty and peculiarity. Fortunately, there have been a number of efforts using hemispherical photographs to assess the effect of obstruction on irradiation (Anderson 1964, Koike 1985, Wang et al. 1992, Fournier et al. 1996, Saito 1996). These provide us a method using hemispherical photographic silhouette to estimate the optical porosity in a coastal protective forest, and further to assess the relationships between wind speed and optical porosity within the coastal protective forest (Zhu et al. 2003).

The objective of this study is to establish a relationship between the optical porosity and relative wind speed in a coastal pine forest stand thinned to different stem densities. First, the definition of optical stratification porosity (OSP) and the method using hemispherical photographic silhouettes for estimating the OSP are introduced briefly. Then, the distributions of OSP and relative wind speed are discussed in the coastal pine forest with different stem densities. Finally, the relationship between relative wind speed and the OSP in the coastal pine forest is examined. Such a relationship could be proved useful in prediction of the wind speed profile within the canopy from relatively simple field measurements of the optical stratification porosity.

2 Material and Methods

2.1 Site Description

The experiments were conducted in a coastal pine forest for sand-control with different stem densities, which were produced by thinning. The site is located at Aoyama shore, Niigata prefecture, Japan, at 37º52 41.3”N, 138º56 16.8”E, on a sandy soil with a slope around 4º. The coastal forest was planted about 35 years ago at a spacing of 1.5 × 1.5 m, to give an initial stocking density of approximately 4500 stems ha^{-1}, and to discourage the development of an understorey. It is composed of Japanese black pine (*Pinus thunbergii* Parl.) and stretches along a road in about 60º from the true north to several kilometers.

There is a 50 m wide zone of young pine trees

Table 1. Mean stand characteristics of the coastal pine forest with four stem densities.

Treatment No.	Diameter at breast height (cm)	Clear bole height (H_0) (m)	Tree height (H) (m)	Density (stem ha^{-1})	Basal area (m^2 ha^{-1})	H_0/H	Thinning rate by stem (%)	Thinning rate by basal area (%)
Before thinning (December 1997)								
1	9.2	3.9	7.5	3217	23.36	0.52	20.2	19.8
2	9.0	3.1	5.9	3167	21.42	0.53	31.6	32.5
3	10.1	4.2	7.3	3000	26.00	0.58	46.7	50.2
4	8.7	3.3	6.2	3600	23.15	0.54	0.0	0.0
Soon after thinning (February 1998)								
1	9.4	3.9	7.5	2517	18.75	0.52		
2	9.1	3.2	5.9	2100	14.46	0.53		
3	10.1	4.3	7.2	1483	12.94	0.59		
4	8.7	3.3	6.2	3600	23.15	0.54		
Two growing seasons after thinning (January 2000)								
1	9.8	4.0	8.5	2517	21.27	0.47		
2	9.8	3.2	7.0	2100	16.91	0.45		
3	10.8	4.1	8.2	1483	15.48	0.49		
4	9.3	3.7	7.2	3600	26.13	0.44		

behind the sand dune along the seashore. The distance from the shoreline to the road, i.e., the front edge of the coastal forest, is about 120 m. The coastal forest was thinned with four treatments in December of 1997, i.e., 20%, 30%, 50% thinned and control (unthinned), which are referred to Treatment 1, Treatment 2, Treatment 3 and Treatment 4, respectively. The area of each treatment was 20×30 m^2, surrounded by a buffer zone in the same treatment so that the effective area reached 40×50 m^2. It is about 80 m from the front edge of the coastal forest to the centers of the treatment plots. The stand characteristics before and after thinning are shown in Table 1.

2.2 Wind Measurement

Wind data (wind speeds and directions) inside and outside the coastal forest were collected after thinning. One propeller anemometer (Tokyo Ota No. 111-T, Kona Ltd. Japan) with a data logger (Kona DS-64K, Kona Sapporo, Japan) was mounted at a height of 2 m above the ground nearby the sea (about 100 m from the see water) for the purpose of obtaining fundamental data outside the coastal forest. In order to observe the distribution of vertical wind speed inside the coastal forest, two observation towers of 10-m height were established in the control plot (unthinned, treatment 4) and the plot with the most intense thinning (treatment 3, 50% thinned).

Two steel pipes fixed with retractable poles of 10-m height were installed in treatment 1 (20% thinned) and treatment 2 (30% thinned). The collection of vertical wind data in the four treatments was conducted during November of 1999 and January of 2000 using two sets of 4-channel hot-wire anemometers (Rion Tr-Am-11, Rion Ldt. Japan) (Table 2). The observed heights were generally in every 1.0 m up to the forest top, of which one sensor was set just above the forest top (Table 2).

The sensors of the hot wire anemometers were mounted on 1.5 m long arms on the towers and 0.4 m long arms on the 10-m height poles. Simultaneously, two propeller anemometers (Young Model 05103-16B, R. M. Young Company, USA) with data loggers (Kona Kadec-Kaze, Kona Ldt. Japan) were mounted on the top of the two towers in order to get continuous wind data. Intervals of wind data collection were 2 minutes or 10 minutes for the propeller anemometers and 0.5 minute for the hot-wire anemometers. Data runs were irregular in length (between 1 and 6 hours for a run) but generally included the later morning and afternoon. All wind speed data were calibrated according to the hot wire anemometer.

For estimating the atmospheric stability, a three-dimensional sonic anemometer (Kaijo

Table 2. Instrument types and heights.

Instrument type	Instrument heights* (m) Treatment No. 1	2	3	4
Hot wire anemometer				
Sensor A-1	1.0	1.0	1.0	1.0
Sensor A-2	2.0	2.0	2.0	2.0
Sensor A-3	3.0	3.0	3.0	3.0
Sensor A-4	4.0	4.0	4.0	4.0
Sensor B-1	5.0	5.0	5.0	5.0
Sensor B-2	6.0	6.0	6.0	6.0
Sensor B-3	7.0	Top 7.0	7.0	Top 7.2
Sensor B-4	Top 8.5	8.0	Top 8.3	8.0
Young Model propeller anemometer	**Nu	Nu	10.6	10.6
Sonic anemometer	Nu	Nu	Nu	10.0
Ota No. 111-T propeller anemometer 2.0 m, outside the forest close to the sea				

* The eight sensors of the hot wire anemometers were amounted at various heights and the wind data were collected simultaneously in each treatment. Sonic anemometer was set on the top of tower in treatment 4 (unthinned) during the collection of vertical wind data in each treatment.
** Nu: Not used.
Top The sensor set just on the canopy top.

Denki DA-600-3TV, Kaijo Cooperation, Japan) was set on the top of the tower in treatment 4 (unthinned) when vertical wind speeds were measured in each treatment (Table 2). Wind velocity components (longitudinal u, lateral v, and vertical w wind velocity) and temperature (T) were sampled and digitized at a rate of 10 Hz by a data-logging system (TR-62TX, Kaijo Cooperation, Japan) with a data appending system controlled by a computer (PC-9801NS/L, NEC, Japan). Instantaneous data were put onto the hard disk of the computer in the field. The computation was based on a time series of 8192 points over an 819.2 s period.

Wind data obtained inside the coastal forest were selected to meet the following criteria:

1) Wind speed of interval average outside the coastal forest was more than 3.0 m s^{-1}.
2) Wind direction of interval average outside the coastal forest was approximately perpendicular to the coastal forest along the road.

If either of these criteria were not met within the interval, the data obtained inside the coastal forest for the period were discarded. Wind speed data obtained in the coastal forest were sorted by height and wind direction, the mean values were computed with the corresponding wind data outside the coastal forest. Consequently, wind data from ten days were found to meet the criteria (Table 3). Wind data from November 11 in treatment 1, November 22 in treatment 2, November 23 in treatment 3 and December 1 and December 8 of 1999 in treatment 4 were used to develop the related models; other data were used to test the obtained models (Table 3).

2.3 Optical Stratification Porosity (OSP)

2.3.1 Definition of the OSP

Stratification porosity is used to describe the distribution of pores of a forest stand on a vertical profile of forest stand. That is, assuming to cut a forest stand horizontally into many slabs in vertical direction, then the porosity of each slab is recognized as the stratification porosity. However, it is almost impossible to physically measure the aerodynamic porosity (Loeffler et al. 1992). Therefore, the optical stratification porosity (OSP), a two-dimensional measure of stratification porosity determined from forest silhouettes in vertical direction, is adopted as an alternative of the stratification porosity. The optical stratification porosity is defined as the proportion of sky hemisphere not obscured by tree elements downward the horizontal plane at a given height inside a forest stand. An individual OSP can be determined as the ratio of the pore

Table 3. The fundamental characteristics of wind data used to develop and test models.

Treatment No.	Date and period (GMT+09:00)		Hot wire anemometer inside the coastal forest				Propeller anemometer outside the coastal forest			
		Interval (s)	Maximum velocity [a] at the top of canopy (m s^{-1})	Mean velocity [b] at the top of canopy (m s^{-1})	Mean friction velocity [c] (m s^{-1})	Mean atmospheric stability (H/L) [d]	Interval (s)	Maximum velocity (m s^{-1})	Mean velocity (m s^{-1})	Mean wind direction (true north degree)
1	Nov. 11 1999 10:09-14:50	M 30	5.9	3.2	0.74	0.0006	120	6.0	4.7	344
	Jan. 29 2000 09:15-11:30	T 30	7.6	4.1	0.96	0.0005	600	8.4	6.6	353
2	Nov. 22 1999 09:50-15:50	M 30	5.4	3.0	0.69	0.0007	120	8.5	6.4	330
	Dec. 10 1999 11:15-15:00	T 30	8.1	4.6	1.30	0.0003	600	10.0	8.1	299
3	Nov. 23 1999 13:30-14:30	M 30	7.8	4.7	1.29	0.0002	600	11.6	9.5	327
	Dec. 27 1999 11:30-15:10	30	5.4	2.3	0.57	0.0014	600	6.4	4.3	17
4	Dec. 01 1999 13:28-15:10	M 30	3.2	1.6	0.26	0.0031	600	6.5	4.8	360
	Dec. 08 1999 11:30-15:00	M 30	7.5	4.3	1.07	0.0002	600	11.4	9.8	330
	Dec. 09 1999 12:30-13:30	T 30	8.8	4.5	1.13	0.0001	600	11.4	10.3	293
	Dec. 24 1999 15:40-16:40	T 30	5.1	2.9	0.65	0.0009	600	8.6	7.6	283

[a] Maximum velocity: the maximum value in the interval.
[b] Mean velocity: the overall mean value during the period.
[c] Mean friction velocity: obtained at the top of the tower in treatment 4 (unthinned treatment), z = 10 m.
[d] H / L : H is mean tree height in treatment 4 (unthinned stand), H = 7.2 m. L is Monin-Obukhov length (m), which was calculated as follows: $L = Tu^{*3} / \kappa g \overline{w'T'}$, $u^* = \sqrt{-\overline{u'w'}}$
where u' is longitudinal velocity fluctuation (m s^{-1}), and w' is vertical velocity fluctuation (m s^{-1}); T is temperature (K), g is gravity accelerator (m s^{-2}), $\overline{w'T'}$ is heat flux (W m^{-2}).
M Wind data used for developing the related models, and T Wind data used for testing the related models.

area to the total area using the forest silhouettes in vertical direction on a horizontal plane (Zhu et al. 2003).

The hemispherical photography is a suitable tool for studying the canopy architecture and light regime of forest environments. It has been proven useful in studies requiring fine details of canopy structure or the light penetration (Chen and Black 1991). In addition, it combines the advantages of relatively simple procedure for data acquisition, good spatial definition of imagery and the easily processing system for the image (Fournier et al. 1996). Therefore, the hemispherical photographic silhouette was used for OSP estimation in this experiment. In fact, the optical porosity is not equal to the effective porosity or aerodynamic porosity because the optical porosity shows only the two dimensional gaps. Nevertheless, the optical porosity has frequently served as a descriptor of natural plants for lack of a practical alternative (Heisler and DeWalle 1988).

2.3.2 Measurement of the OSP

The OSP was measured using a digital hemispherical camera (Nikon, Coolpix 910, Japan, f = 7~21 mm) with a 180º fish-eye converter lens (Nikon, FC-E8, Japan, f = 1.7 mm) on calm days soon after the observation of wind in the four treatments. The fish-eye lens provided with a simple polar projection of the tree elements. In order to take the photographs at a given height, the camera with the fish-eye lens was set into a control-box and fixed vertically on the top of a retractable pole, which was extendible more than 10 m upward. The observed heights for estimation of OSP were in an interval of 1.0 m from the forest floor up to the canopy top and at least three successful images were taken at each height. The images were recorded to a built-in compact flash card. Adobe-Photoshop software was chosen as the image processing system. The software provided the total pixels of a given image and the total pixels of tree elements in the same image. Therefore, the value of OSP at a given height can be estimated from Eq. 1.

$$P_z = S_z / S_{Tz} \quad (1)$$

where P_z is optical stratification porosity at height z, which is estimated from the hemispherical image (non-dimension), S_z is area of pores in a given image (pixels), S_{Tz} is the total area of the processed image (pixels). Up to three images were available for analysis of OSP for each height, OSP was determined separately for each image and then average value for each height was computed.

3 Results

3.1 Distribution of Optical Stratification Porosity

3.1.1 Distribution of OSP in Theory

According to the definition of OSP, it increases with the increment of height in a forest stand, and attains the maximum 1.0 (the pore proportion is 100%) when it reaches at or over the top of the forest stand. Contrarily, OSP with a value of 1.0 at the top of the forest stand decreases gradually downwards. On the basis of the principle of light attenuation, i.e., the Lambert-Beer's law (Yasugi et al. 1996), the OSP can be obtained under the assumption of homogeneous distributions of branch, leaf and stem in the forest stand (Eq. 2).

$$\ln(P_z / P_0) = -\nu d \quad (2)$$

where d is a distance of the light beam through the homogeneous medium (m), ranging $0 \le z \le H$. H is top height of the forest stand (m). $P_0 = 1.0$ at or over the forest top. ν is a constant called extinction coefficient relating to the change of OSP. Coefficient ν should be a constant and independent on distance under the assumption of homogeneous distribution of tree elements.

Solving Eq. 2,

$$P_z = P_0 \exp(-\nu d) \quad (3)$$

If the zenith angle of the beam reaching the camera is θ, the distance of a beam light reaching the horizontal plane will become

$$z = d/\cos(\theta) \quad (4)$$

Table 4. Regression statistics for determination of the relationships between zenith angle and OSP in treatment 1 (The same as treatment 2, 3 and 4) ($\ln(P_\theta) = -\beta_s x$).

	Height (m)						
	1	2	3	4	5	6	7
R^2	0.78	0.74	0.55	0.53	0.71	0.84	0.80
Constant β_s	0.331	*0.370	0.306	0.244	0.217	0.188	0.074
Standard error	0.063	0.077	0.089	0.093	0.056	0.047	0.029
t-value	–5.254	–4.805	–3.438	–2.624	–3.875	–4.000	–2.552
Significance *p*	0.000	0.000	0.001	0.002	0.001	0.002	0.004

The data used to estimate parameter β_s were from the images obtained at each height, which calculated from seven equiangular circle-belts with three repeats.
* β_s value at height 2.0 m was larger than at 1.0 m may be caused by the errors from the measurement of OSP in the field.

Combining Eqs. 3 and 4,

$$P_{z\,\theta} = P_0 \exp[-\nu\, z / \cos(\theta)] \quad (5)$$

where $P_{z\,\theta}$ is the OSP related to height and the zenith angle of view.

3.1.2 Determination of Standard OSP

In most of the images taken in the deeply shaded points, the image area above a certain degree of zenith was usually black. In order to compare the OSP among stands with different stem densities, the relationship between OSP and the zenith angle was examined. On the assumption that parameter ν (Eq. 5) is constant, the OSP at a given height z is determined only by zenith angle (θ). The OSP decreases with the increment of zenith angle because the silhouette is a polar projection. If the canopy edge of a forest stand is limited to a certain range, the OSP will be changed abruptly when the zenith angle increases to cover the range exceeding the canopy edge. While, if the canopy edge of a forest stand is unlimited, the OSP will decrease with the increasing of zenith angle of the view (θ) as expressed in Eq. 5 (Zhu et al. 2003). Because the hemispherical photographs were taken in the coastal forest stand with unlimited canopy edge, it is possible to test the effect of the zenith angle (θ) on the estimation of OSP by dividing the image into equiangular circle-belt. Eq. 5 can be written in a simple form (Eq. 6), if $\nu z = \beta_s$ and $x = 1/\cos(\theta)$,

$$P_\theta = P_0 \exp(-\beta_s x) \quad (6)$$

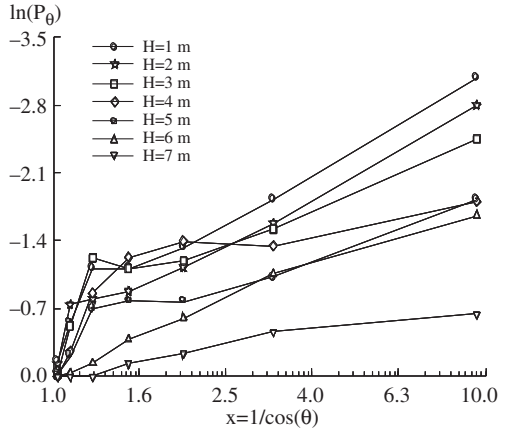

Fig. 1. Relationship between OSP and zenith angle at different heights in treatment 1 (The data were also used in Zhu et al. 2003).

$$\ln(P_\theta) = -\beta_s x \quad (7)$$

where P_θ is the OSP at a certain height (non-dimension).

In order to determine the standard or uniform area of image for SOP estimation, the images taken from treatment 1 (20% thinned) at each height were divided into seven equiangular circle-belts. The variation of OSP with zenith angle (θ) from treatment 1 was plotted in Fig. 1 ($\ln(P_\theta)$ against x). The tested result was listed in Table 4. The result suggests that when the zenith angle (θ) is more than 0.46π, the OSP in the circle-belt was nearly constant to 0. Therefore, the OSP was calculated for a sub-circle 80º of zenith (three-quarter area of the hemispherical image) to minimize the influence of underexposed areas and to

allow comparisons among the different thinning treatments. The three-quarter area porosity with excluding the outer one-quarter is determined as the standard OSP.

3.1.3 Distribution of OSP (Standard)

The distributions of OSP measured in the coastal pine forest with different thinning ratios are showed in Fig. 2. The result indicates that OSP is relative stable in the trunk layer and changes greatly within the canopy layer (the trunk layer and canopy layer were divided by bole height, H_0). Obvious differences existed across the thinning ratios in the coastal forest. The OSP under the bole height ranged between 0.192~0.213 for treatment 4 (unthinned), 0.252~0.315, 0.281~0.344 and 0.367~0.418 for treatment 1 (20% thinned), treatment 2 (30% thinned) and treatment 3 (50% thinned) respectively (Fig. 2). This ranking exactly follows the ranking of stem densities in the four treatments.

It is obvious that in the single-even-aged coastal forest, two layers can be divided by the bole height (H_0). If the distribution of OSP is expressed by relative height, according to Eqs. 2 and 3, the distribution of OSP in the coastal forest can be written as,

$$P_z = P_0 \exp[-\nu_c(1 - z / H)] \quad (H_0 \le z \le H) \tag{8}$$

$$P_z = P_0 \exp[-\nu_c(1 - H_0 / H) - \nu_t(H_0 / H - z / H)] \quad (0 \le z < H_0) \tag{9}$$

where parameters of ν_c (canopy layer) and ν_t (trunk layer) are coefficients relating to the change of OSP, they should be constant and independent on distance under the assumption of homogeneous distribution of tree elements in each layer. The parameters of ν_c and ν_t were obtained using the measured OSP (Fig. 2), and their fitness were tested and listed in Table 5.

The comparison between predicted OSP by the models (Eqs. 8 and 9) and the measured in field is showed in Fig. 3. No significant difference has been found between the predicted and the measured OSP for each treatment at $p < 0.005$ level.

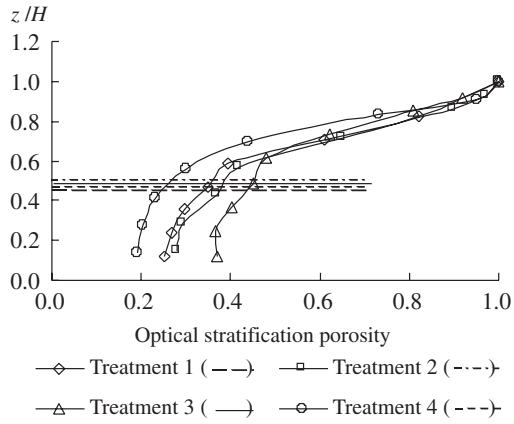

Fig. 2. Distribution of optical stratification porosity obtained from the coastal pine forest with different thinning intensities. The legend of bole height mark is in the bracket (Data in this figure were also used in Zhu et al. 2003).

3.2 Relative Wind Speed Profiles

3.2.1 Basic Characteristics of Wind

The fundamental characteristics of the wind data used in this analysis are listed in Table 3. An order-of-magnitude of stability length (Monin-Obukhov length) (L) (see Table 3) was calculated from the measurements of sonic anemometer. Assuming that displacement height of logarithm law was the order of magnitude of tree height, the stability length L was found to be the order of more than 1000 m for most of the measurements, therefore, the atmospheric stability was usually neutral in the experiment.

3.2.2 Distribution of Relative Wind Speed within the Canopy

The analytical model for air movement within plant canopies developed in the literature (Plate 1971, Bergen 1971, Landsberg and James 1971, Konda and Akashi 1976, Ciono 1985) equates the canopy to a two-dimensional distribution of infinitesimal momentum sinks corresponding to the canopy surfaces (Bergen 1971). The model

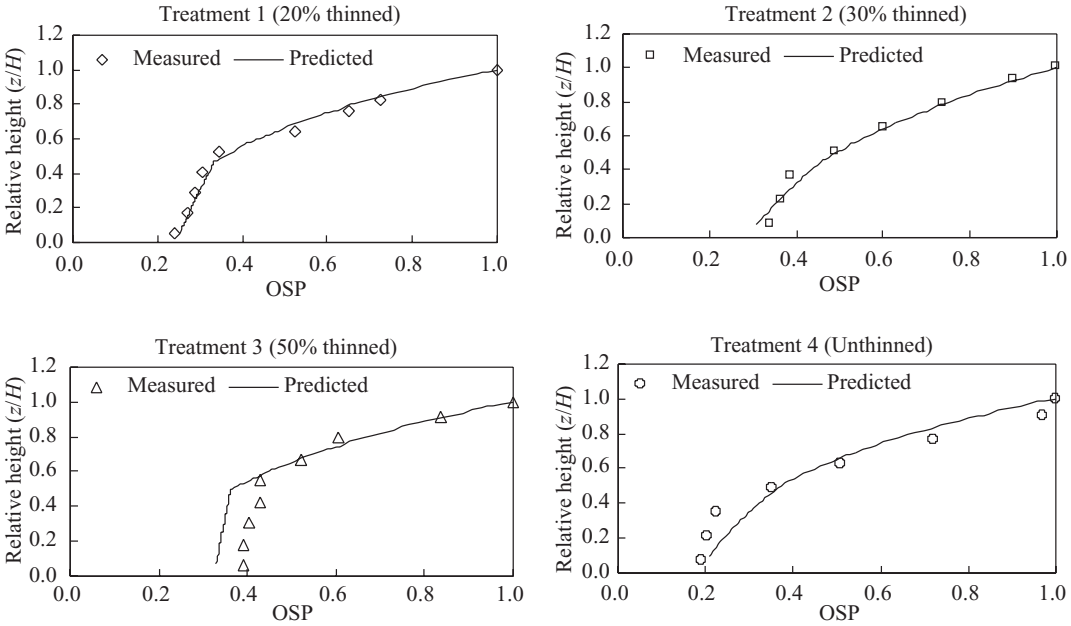

Fig. 3. Comparison between predicted and measured OSP for the coastal pine forest with different stem densities (Data in this figure were also used in Zhu et al. 2003).

Table 5. Regression statistics for determination of the coefficient ν in the OSP model by dividing the stand into canopy layer and trunk layer.

	Thinning treatments							
	Treatment 1		Treatment 2		Treatment 3		Treatment 4	
	Canopy layer	Trunk layer	Canopy layer	Trunk layer	Canopy layer	Trunk layer	Canopy layer	Trunk layer
R^2	0.973	0.935	0.934	0.815	0.982	0.829	0.969	0.991
Constant ν_c, ν_t	1.97	0.24	1.76	0.68	1.67	1.06	2.54	1.40
Standard error	0.077	0.009	0.014	0.011	0.003	0.011	0.050	0.005
t-value	–25.584	–26.667	–125.714	–61.818	–556.667	–96.364	–50.800	–280.000
Significance *p*	0.000	0.003	0.000	0.000	0.000	0.000	0.003	0.001

Parameters of ν_c and ν_t were determined by data from OSP observations, which were made in an interval of 1.0 m from the forest floor up to the canopy top with three repeats.

of airflow within canopies was formulated as exponential function of height in Eq. 10.

$$U_{in(z)} = U_H \exp[-\alpha(1 - z / H)] \quad (10)$$

where z is the interest height within the canopy (m), H is height of top of tree canopy (m), U_H is wind speed (m s^{-1}) at height H, $U_{in(z)}$ is wind speed (m s^{-1}) at height z within the canopy, coefficient α is a constant called attenuation coefficient (Amiro 1990) or canopy flow index (Cionco 1985, Groß 1993). The coefficient α, which is related to drag coefficient and average foliage density (Landsberg and James 1971, Kondo and Akashi 1976, Cionco 1985), determines the form of wind profile within a wide variety of vegetation canopies. The wind profiles within the canopy could be compared quantitatively among the various thinning ratios using the attenuation coefficient α.

The mean profiles of relative wind speed obtained from November 11, November 22, November 23 and December 1 and 8 for treatment 1, treatment 2, treatment 3 and treatment 4, respectively were showed in Fig. 4. The regres-

sion statistics for determination of coefficient of α in Eq. 10 were shown in Table 6. The exponential relationships were found with α = 3.21 for treatment 4 (unthinned), α = 2.43, 2.05 and 1.77 for treatment 1 (20% thinned), treatment 2 (30% thinned) and treatment 3 (50% thinned), respectively. The reduction of tree density through thinning causes the changes of the vertical forest structure. It is the change that causes the differences of wind profiles within the canopy among the stands with various thinning ratios. Therefore, it can be concluded that greater attenuation of wind speed is related to the canopy density in the various thinning ratios.

The comparison between wind profiles calculated from the model (Eq. 10) with the attenuation coefficients (Table 6) and that measured in field (wind data measured on January 29 of 2000 for treatment 1, December 10 of 1999 for treatment 2, December 27 of 1999 for treatment 3 and December 9 and 24 of 1999 for treatment 4) is showed in Fig. 5. No significant difference has been found between the wind profiles from predicted and measured for each treatment at $p < 0.01$ level.

3.2.3 Relative Wind Speed in the Trunk Space

In the trunk layer (under the canopy), the wind profiles were not fitted the exponential form because of the second maximum appearance of wind speed, i.e., the "blow-through" phenomenon, which may be due to the larger gap, occurring in the trunk layer, especially in treatment 3 (50% thinned). The distributions of the wind profiles (mean values of $U_{in(z)} / U_H$) for the four treatments were shown in Fig. 4.

4 Discussion

4.1 Relationship between OSP and Relative Wind Speed

The relationships between the optical stratification porosity and relative wind speed are plotted in Fig. 6. The linear relationships between optical stratification porosity and the relative wind speed ($R_w = U_{in(z)} / U_H$) within the canopy are clearly shown for all the four treatments (Fig. 6A). However, it seems to be little correlated to each other in the trunk layer (Fig. 6B).

As analyzed above, both distributions of wind profile and the OSP are influenced by the tree ele-

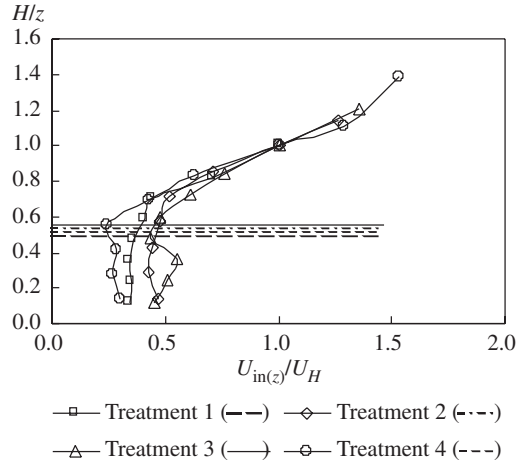

Fig. 4. Mean wind profiles in the four treatments. The legend of bole height mark is in the bracket. Wind data used in this figure were obtained on November 11, November 22, November 23 and December 1 and 8 of 1999 for treatment 1, treatment 2, treatment 3 and treatment 4, respectively.

Table 6. Regression statistics for determination of coefficient of α in Eq. 10.

	Total average in each treatment			
	Treatment 1	Treatment 2	Treatment 3	Treatment 4
R^2	0.898	0.952	0.902	0.981
Coefficient α	2.43	2.05	1.77	3.21
Standard error	0.170	0.050	0.130	0.200
t-value	–14.294	–41.000	–13.615	–16.050
Significance *p*	0.005	0.000	0.007	0.004

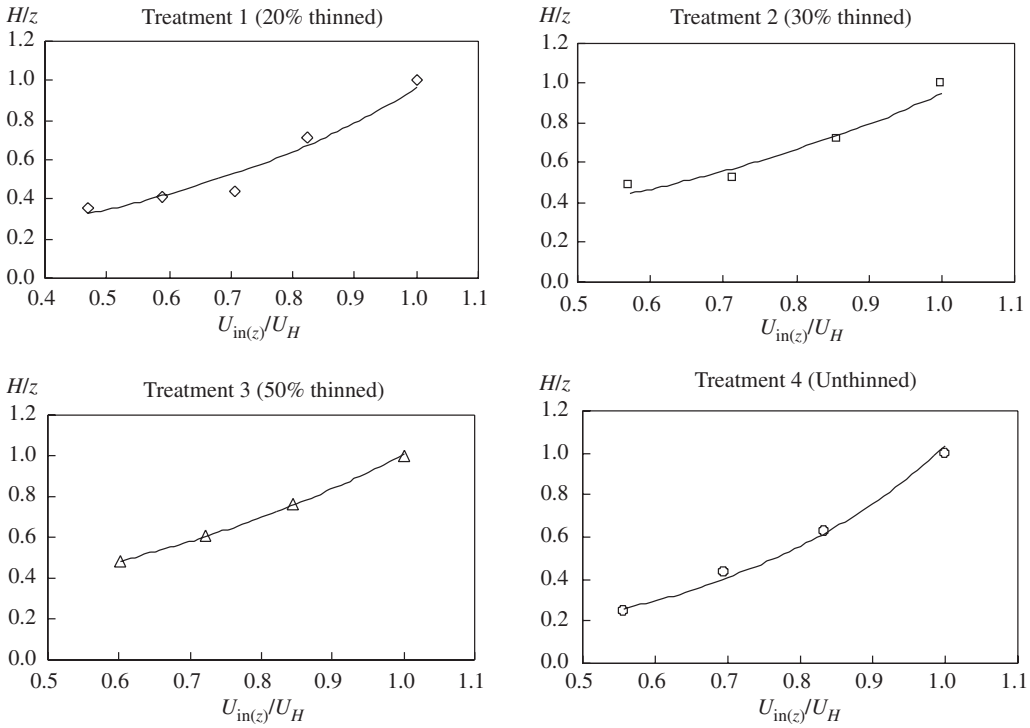

Fig. 5. Comparison between predicted and measured wind profiles within the canopy for the coastal pine forest with different thinning intensities. Wind data were measured on January 29 of 2000 for treatment 1, December 10 of 1999 for treatment 2, December 27 of 1999 for treatment 3 and December 9 and 24 of 1999 for treatment 4, respectively.

ments (leaves, branches and stems) in the forest stand, in particular within the canopy (Fig. 6A). Therefore, relative wind speed within the canopy could be predicted from the distribution of OSP. Regression analysis showed that OSP was the independent variable that significantly contributed to predicting the relative wind speed within the canopy. The regression equation obtained as

$$R_w = aP_z + b \quad (11)$$

where $R_w = U_{in(z)} / U_H$, the relative wind speed, a and b are coefficients determined from the measurements of wind and OSP.

The coefficients a and b in the linear regression Eq. 11 were determined based on the wind data obtained from November 11, November 22, November 23 and December 1 and 8 for treatment 1, treatment 2, treatment 3 and treatment 4, respectively in Fig. 7.

Comparing the two profiles of OSP and wind velocity within the canopy, we found that they had the same form (Eqs. 8, 10) and they are determined by the coefficients α and ν respectively. Therefore, it is significant to check the relationship between the two coefficients of wind profile (α) and the distribution of OSP (ν) within the canopy. The relationship between the two coefficients is examined (Fig. 8). A consistent relationship is found between the parameters of α and ν, and can be expressed as

$$\alpha = 1.5855\nu - 0.7821 \quad (12)$$

$(R^2 = 0.98, p < 0.005)$

Based on this relationship, the attenuation coefficient α of wind profile can be simply estimated from the measurement of OSP. The measurement of OSP is relatively easy because the estimation

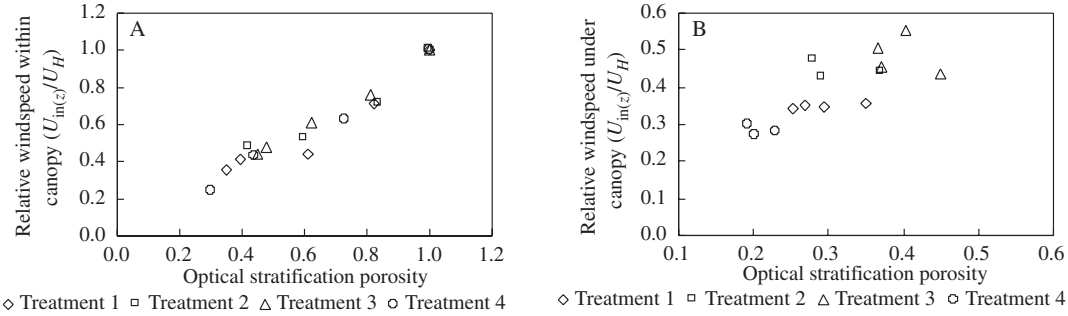

Fig. 6. Relationships between relative wind speed and OSP for the coastal pine forest with different stem densities. A: within the canopy, B: under the canopy.

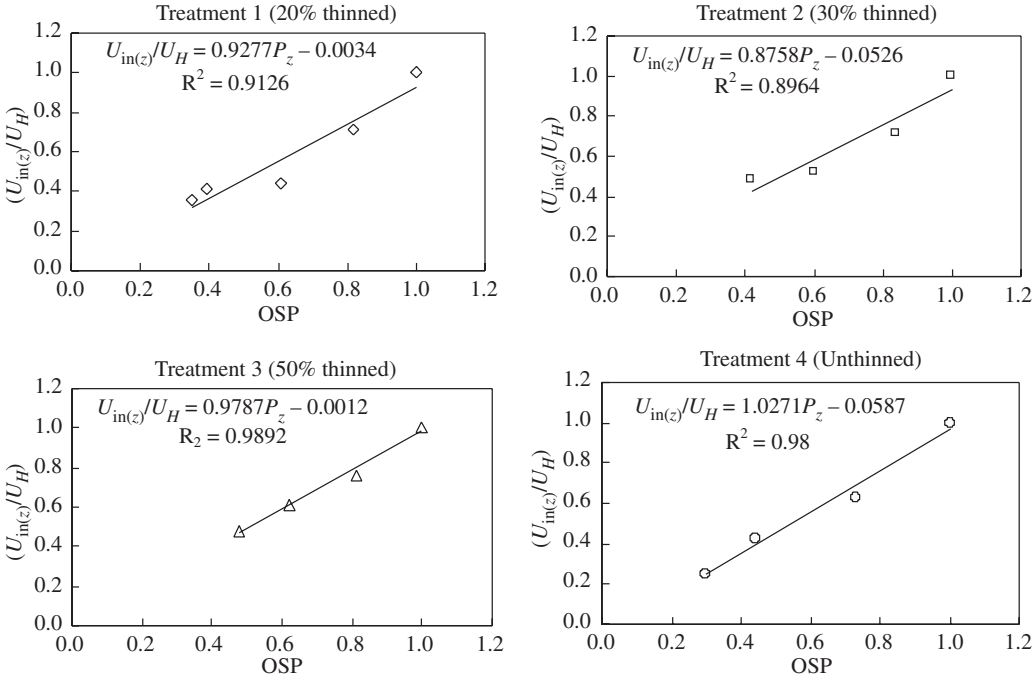

Fig. 7. Regressions of relative wind speed and OSP within the canopy for the coastal pine forest with different stem densities.

of parameter ν within the canopy requires images of photographs at only one position.

In the situation of trunk layer, the distribution of OSP also followed the Lambert-Beer s law although it was relatively constant (Fig. 2). However, the wind profiles were not fitted the exponential form there because of the "blow-through" phenomenon. Therefore, relative wind speed was little correlated with the distribution of OSP there, and the relative wind speed in the trunk layer could not be predicted directly from the OSP.

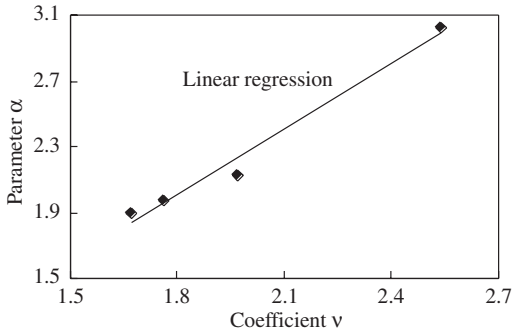

Fig. 8. Relationship between parameters of α and ν used in wind profiles and the distribution of optical stratification porosity within the canopy.

4.2 Estimation of Profiles of Relative Wind Speed within the Canopy from OSP

The wind data measured on January 29 of 2000 for treatment 1, December 10 of 1999 for treatment 2, December 27 of 1999 for treatment 3 and December 9 and 24 of 1999 for treatment 4, respectively are showed in Fig. 9.

The predicted relative wind speeds using Eq. 11 are also showed in Fig. 9 (the solid line, Predicted 1). The differences (mean value ± standard error) between the predicted and measured are 0.0648 ± 0.0331, 0.0656 ± 0.0088, 0.0166 ± 0.0129 and 0.0336 ± 0.0241 for treatments 1, 2, 3 and 4, respectively. It can be concluded that these differences between the predicted and measured values can be ignored when predicting the relative wind speed using the linear relationship between OSP and relative wind speed within the canopy.

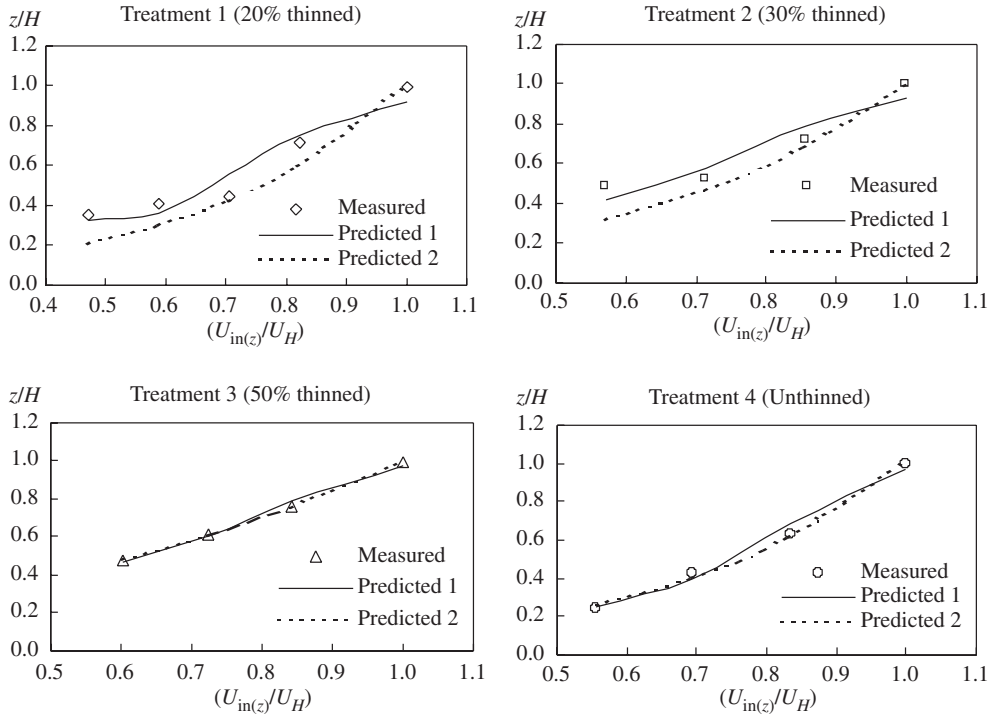

Fig. 9. Relative wind speeds within the canopy predicted from linear relationships between OSP and relative wind speed and between parameters of α and ν. Solid line, Predicted 1 was predicted from the linear regression in Eq. 11; dash line, Predicted 2 was predicted from the linear regression in Eq. 12. The measured wind data were measured on January 29 of 2000 for treatment 1, December 10 of 1999 for treatment 2, December 27 of 1999 for treatment 3 and December 9 and 24 of 1999 for treatment 4, respectively.

The relative wind speeds within the canopy predicted from Eq. 10 by using coefficient α, which is estimated from Eq. 12, are also plotted in Fig. 9 (the dash line, Predicted 2). The differences (mean value ± standard error) between the predicted and measured are also examined, i.e., 0.0836 ± 0.0653, 0.0644 ± 0.0072, 0.0058 ± 0.0057 and 0.0169 ± 0.0118 for treatments 1, 2, 3 and 4, respectively. Besides treatment 1, the differences are less than those predicted from Eq. 11. Therefore, Eq. 12 can also provide good fitness in predicting the relative wind speed within the canopy.

5 Conclusions

We have adopted this definition of optical stratification porosity in developing the models because of the relative easiness and accuracy of the measurement, and it permits comparison among different forest stands. The results suggest that optical stratification porosity can be used to predict the relative wind speed within the canopy of coastal pine forests. Therefore, it may be useful as a guide in the field evaluation of the coastal protective plantation for fine-scale ecology study.

The regression results indicate that the higher predictive accuracy could be achieved if enough OSP data were available to develop the prediction equations. However, the relationships derived in this paper should be applied only to the conifer forests. In the case of coniferous forest, the distribution of needles, clusters and branches is relatively homogeneous within the canopy, the linear relationship between the alternative of the aerodynamic porosity, i.e., the OSP, and wind speed has been established successfully. Although it has not been verified for the situation of other tree species in this study, it is possible to obtain the relationships between the OSP and wind speed profile within the canopy for other tree species using the procedures provided in this paper.

Acknowledgements

We would like to thank Professor Tomohiko Kamitani for providing stand information, and for his valuable suggestions. We also gratefully acknowledge Professor Fengqi Jiang for his valuable comments. Thanks are also due to Professor Dali Tao and Dr. Professor Dehui Zeng for their checking the English manuscript. We also thank Mr. Kenji Sakioka and Mr. Hirotaka Yamazaki for their help in data collection. Special thanks go to the Department of Forest, Erosion Control Laboratory, Tokyo University for the loan of the sonic anemometer. This study was supported by the innovation research project of the Chinese Academy of Sciences (KZCX3-SW-418) and Monbusho of Japan government.

References

Amiro, B.D. 1990. Comparison of turbulence statistics within three boreal forest canopies. Boundary-Layer Meteorology 51: 99–121.

Anderson, M.C. 1964. Studies of the woodland light climate, 1. The photographic computation of light conditions. Journal of Ecology 52: 27–41.

Bean, A., Aloeri, R.W. & Federer, C.A. 1975. A method for categorizing shelterbelt porosity. Agricultural Meteorology 14: 417–429.

Bergen, J.D. 1971. Vertical profiles of wind speed in a pine stand. Forest Science 17: 314–321.

Blackburn, P. & Petty, J.A. 1988. Theoretical calculations of the influence of spacing on stand stability. Forestry 61: 235–244.

Cao, X.S. 1983. Shelterbelts for farmland. Chinese Forestry Press, Beijing. 645 p. (in Chinese).

Carborn, J.M. 1965. Shelterbelts and microclimate. Faber and Faber Ltd. London, 288 p.

Cionco, R.M. 1985. Modeling wind fields and surface wind profiles over complex terrain and within vegetation canopies. In: Hutchison, B.A. & Hicks, B.B. (eds.). The forest-atmosphere interaction. D. Reidel publishing company, Boston, Lancaster, p. 501–520.

Chen, J.M. & Black, T.A. 1991. Evaluation of hemispherical photography for determining plant area index and geometry of forest stand. Agricultural

and Forest Meteorology 56: 129–143.

Ennos, A.R. 1997. Wind as an ecological factor. Trends in Ecology & Evolution 12: 108–111.

Fournier, R.A., Landry, R., August, N.M., Fedosejevs, G. & Guuther, R.P. 1996. Modeling light obstruction in three conifer forests using hemispherical photography and fine tree architecture. Agricultural and Forest Meteorology 82: 47–72.

Fu, M.H., Jiang, F.Q. & Yang, R.Y. 1992. Study on porosity of poplar shelterbelt and its application in tending and felling. In: Jiang, F.Q. (ed). Management techniques and theoretical basics for shelterbelts. Chinese Forestry Press, Beijing. p. 102–108. (in Chinese with English abstract).

Groß, G. 1993. Numerical simulation of canopy flows. Springer-Verlag, Berlin, Heideberg, Now York, London, Paris, Tokyo, Hong Kong, Barcelona, Budapest. 166 p.

Hagen, L.J. & Skidmore, E.L. 1971a. Windbreak drag as influenced by porosity. Transactions of the ASAE 14: 464–465.

— & Skidmore, E.L. 1971b. Turbulence velocity fluctuations and vertical flow as affected by windbreak porosity. Transactions of the ASAE 14: 634–637.

Heisler, G.M. & DeWalle, D.R. 1988. Effects of windbreak structure on wind flow. Agriculture Ecosystems and Environment 22/23: 41–69.

Peltola, H. & Kellomäki, S. 1993. A mechanistic model for calculating windthrow and stem breakage of Scots pines at stand edge. Silva Fennica 27: 99–111.

— , Kellomäki, S., Väisanen, H. & Ikonen, U.P. 1999. A mechanistic model for assessing the risk of wind and snow damage to a single tree and stands of Scots pine, Norway spruce and birch. Canadian Journal of Forest Research 29: 261–267.

Jiang, F.Q., Xu, J.Y., Fu, M.H. & Liu, Z.G. 1989. Determination of shelterbelt porosity by digital image processing. In: Xiang K.F. (ed). Protective plantation technology. Publishing house of Northeast Forest University, Harerbin, p. 366–370. (in Chinese with English abstract).

— , Zhou, X.H., Fu, M.H., Zhu, J.J. & Lin, H.M. 1994. Shelterbelt porosity model and its application. Chinese Journal of Applied Ecology 5: 251–255. (in Chinese with English abstract).

— , Zhu, J.J. & Zhou, X.H. 1999. Model of continuous economic effects of shelterbelts and its applications. Scientia Silvae Sinicae 35: 16–21. (in Chinese with English abstract).

Kenney, W.A. 1987. A method for estimating windbreak porosity using digitized photographic silhouettes. Agricultural and Forest Meteorology 39: 91–94.

Koike, F. 1985. Reconstruction of two-dimensional tree and forest canopy profiles using photographs. Journal of Applied Ecology 22: 921–929.

Kondo, J. & Akashi, S. 1976. Numerical studies on the two-dimensional flow in horizontal homogeneous canopy layers. Boundary-Layer Meteorology 10: 255–272.

Landsberg, J.J. & James, G.B. 1971. Wind profiles in plant canopies: studies on an analytical model. Journal of Applied Ecology 8: 729–741.

Loeffler, A.E., Gordon, A.M. & Gillespie, T.J. 1992. Optical porosity and wind speed reduction by coniferous windbreaks in Southern Ontario. Agroforestry System 17: 119–133.

Moysey, E.B. & McPherson, F.B. 1966. Effect of porosity on performance of windbreaks. Transactions of the ASAE 9: 74–76.

Plate, E.J. 1971. The aerodynamics of shelter belts. Agricultural Meteorology 8: 203–222.

Saito, T. 1996. Relationship between the profiles of wind velocity and gap fraction recorded by hemispherical photographs in a deciduous forest. Journal of Forest Research, Japan Forestry Society 78: 384–389. (in Japanese with English abstract).

Wang, Y.S., Miller, D.R., Welles, J.M. & Heisler, G.M. 1992. Spatial variability of canopy foliage in an Oak forest estimated with fisheye sensors. Forest Science 38: 854–865.

Yasugi, R., Kozeki, H., Furutani, M. & Hitaka, T. 1996. Biology dictionary. Iwanami Shoten Press, Tokyo, Japan. 2027 p. (in Japanese).

Zhou, X.H., Jiang, F.Q. & Zhu, J.J. 1991. Study on random error of shelterbelt porosity estimated by measuring photo with the help of digitized photographic silhouettes. Chinese Journal of Applied Ecology 2: 193–202. (in Chinese with English abstract).

Zhu, J.J. & Jiang, F.Q. 1992. Management basics and sustainable regeneration pattern for shelterbelts or windbreaks. In: Proceeding of China association for science and technology, First annual meeting of youth, volume agriculture, Science and technology press of China, Beijing. p. 76–83. (in Chinese with English abstract).

— , Matsuzaki, T., Sakioka, K. & Yamamoto, M. 1998. Wind speed in a coastal forest belt of Japa-

nese black pine (Pinus thunbergii Parl.) –Vertical wind profile–. Transactions of the Japan Forestry Society 109: 455–458.

— , Matsuzaki, T. & Gonda Y. 2003. Optical stratification porosity as a measure of vertical canopy structure in a Japanese coastal forest. Forest Ecology and Management 173: 89–104.

Total 35 references